American Journal of Geographic Information System 2022, 11(1): 1-8
DOI: 10.5923/j.ajgis.20221101.01

Enhancing Vertical Accuracy of Global Digital Elevation Models for Coastal and Environmental Applications: A Case Study in Egypt

Gomaa M. Dawod[1,*], Ahmed M. Amin[2]

[1]Geodesy Department, Survey Research Institute, National Water Research Center, Giza, Egypt
[2]GIS Department, Survey Research Institute, National Water Research Center, Giza, Egypt

Abstract A major source of Digital Elevation Models (DEM) is the open-source Global DEM (GDEM) developed and distributed free-of-charge and, thus, became accepted in a wide range of coastal end environmental applications worldwide. The vertical accuracy of such GDEMs should be investigated to determine their applicability for utilization in specific activities. Moreover, increasing the vertical accuracy of GDEMs should be carried out by the integration of local terrestrial geodetic datasets over a spatial region. The current study investigates the accuracy of three GDEM models over the Egyptian costs along the Mediterranean sea and tries to enhance such accuracy by adding terrestrial data through the utilization of two methods of spatial modelling within a Geographic Information Systems (GIS) environment. Based on the available datasets and attained results, it has been found that the regression modelling method results in enhancing the vertical accuracy of the investigated GDEMs by 15% and 4% while the krigging geostatistical method produced 24% and 16% improvements. Furthermore, it has been concluded that adding terrestrial local datasets to a global DEM could considerably increase its overall vertical accuracy. However, the number of added terrestrial points should be appropriate to the desired level of vertical accuracy and the area of study. Moreover, it has been concluded that the achieved vertical accuracy of the enhanced models, herein, could be suitable for small-scale mapping and overall management of coastal regions, but it might not be appropriate for accurate environmental studies such as Sea Level Rise (SLR) monitoring and risk assessment which requires a more accurate DEM.

Keywords DEM, Global DEM, Vertical Accuracy, Coastal Management, GIS, Egypt

1. Introduction

A Digital Elevation Model (DEM) is a 3D digital illustration of the Earth's topography. It can be developed in several ways based on the utilized input data. A DEM could be constructed by scanning and digitizing contour maps, by using terrestrial surveys of traditional spirit levelling or by Global Navigation Satellite Systems (GNSS) data. Also, a DEM could be generated from stereoscopic aerial photographs, stereoscopic satellite imageries, and Light Detection and Ranging (LiDAR) measurements. Recently, a DEM can be generated from data obtained by drones equipped with GNSS or LiDAR sensors. Another valuable source of DEM is the open-source Global Digital Elevation Models (GDEM) developed and provided free-of-charge organizations. That source became accepted in a wide range of applications worldwide due to its easy availability.

* Corresponding author:
dawod_gomaa@yahoo.com (Gomaa M. Dawod)
Received: Mar. 15, 2022; Accepted: Apr. 8, 2022; Published: Apr. 15, 2022
Published online at http://journal.sapub.org/ajgis

GDEMs have been utilized in several types of civil and environmental applications such as designing water reservoirs [1], geoids modelling [2], topographic mapping [3], climate change assessment [4], coastal protection [5], flash flood assessment [6], and land subsidence monitoring [7]. The most-critical question dealing with GDEMs concerns their level of vertical accuracy. To judge such an accuracy level, several approaches have been proposed. Examples of such evaluation ways is the assessment utilizing a high-resolution high-accuracy local DEM [8], the utilization of Differential Global Positioning System (DGPS) terrestrial measurements [9], and the comparison with LiDAR-based elevation datasets [10].

GDEMs accuracy level has been investigated in several spatial regions worldwide. For an instant, Dawod and Al-Khamdi [11] have investigated the accuracy of ten GDEMs in both Egypt and the Kingdom of Saudi Arabia (KSA) representing different topography patterns. They reported that such GDEM models produce standard deviations of height differences vary between ± 2.0 m and ± 6.7 m in flat regions, and from ± 4.7 m to ± 18.6 m in mountainous areas. Additionally, Rabah et al. [12] have investigated several GDEMs in Egypt and stated that the overall estimated accuracy range between ± 2.9 m and ± 8.7 m. In India, such accuracy levels range between ± 12.6 and ± 17.8 m [13]. Similarly, Ouerghi et al [14] concluded that the accuracy of some GDEMs in Tunisia vary from ± 7.6 m to ± 10.5 m. In addition, it has been concluded that GDEMs vertical accuracy in China depends on terrain complexity and equal 5 m approximately for plains, 10 m approximately for hills, and 20 m approximately for mountains [15].

Some approaches have been suggested to enhance the vertical accuracy of GDEMs. Rabah et al. [12] stated that some GDEMs utilized a particular Global Geopotential Model (GGM) to convert the originally measured ellipsoidal heights to Mean Sea Level (MSL)-based orthometric heights as the final published product of a GDEM, which is more applicable in civil and environmental applications worldwide. They suggest that replacing those geoidal undulation values with another more-precise GGM would increase the accuracy of a GDEM. Another proposed method considered the utilization of the krigging regression statistical tool to spatially model the GDEM errors [16]. Other researchers suggest filling the gap of a fine-resolution DEM by interpolating their corresponding values from a coarse-resolution one [17,18].

This paper aims to fulfill the following objectives:

- Investigating the vertical accuracy of different resolution GDEMs over the 1000-kilometrs Egyptian coasts along the Mediterranean sea using accurate GNSS/Levelling datasets,
- Studying different mathematical and statistical models for incorporating new data into GDEMs,
- Performing GDEMs enhancement process within a GIS environment in an effortlessly and sensibly manner,
- Analyzing the expected accuracy improvement of different GDEMs by adding a specific number of terrestrial data points,
- Exploring the applicability of enhanced GDEMs for mapping, engineering and environmental applications.

2. Methodology

Two mathematical and statistical techniques have been utilized, herein, to incorporate GNSS/Levelling datasets to the investigated GDEMS, mainly the first-order regression and the ordinary Kriging approaches. Due to their applicability and versatility, both models have been utilized extensively in various geomatics applications. For instance, the first-order regression has been applied to model and predict sea level changes [19]. Also, the Kriging interpolation has been utilized in geoid modelling and refinement [20].

Three GDEM models with variable horizontal resolutions have been investigated herein. The first one is the Shuttle Radar Topography Mission (SRTM 1) model with a resolution of 1 arcsecond or approximately 30 m. SRTMGL1 v. 3 [21] has been utilized herein. (download from e.g. *https://earthexplorer.usgs.gov/*). The second model is the ALOS PALSAR model representing Phased Array type L-band Synthetic Aperture Radar (PALSAR) measurements obtained from the Advanced Land Observing Satellite (ALOS). Its spatial resolution is 12.5 m and could be downloaded from *https://search.asf.alaska.edu/*. ALOS PLASAR (simply PALSAR herein) has been developed by integrating the SRTMGL1 model with the US National Elevation Data (NED) and other datasets and was re-sampled to the 12-m resolution. The datum of the final PLASER is the World Geodetic System 1984 (WGS-84) ellipsoid with the utilization of the Earth Geopotential Model 1996 (EGM96) to convert MSL-based heights to the corresponding ellipsoidal heights [22]. The third GDEM is the Altimeter Corrected Elevations, Version 2 (ACE2 developed by synergistically merging the SRTM data set with Satellite Radar Altimetry within the region bounded by 60°N and 60°S. ACE2 was developed at resolutions of 3, 9 and 30 arc-seconds, and 5 arc-minutes [23]. The 3" ACE2, utilized herein (downloaded from *https://sedac.ciesin.columbia.edu/data/set/dedc-ace-v2*). Although ACE2 is a 90-m resolution model, it produced reasonable accuracy over 1100 GNSS/Levelling checkpoints over Egypt [2].

Table 1. Characteristics of the investigated GDEMs

GDEM	Horizontal Resolution (m)	Height Type	Description
SRTMGL 1	30	Orthometric	A new processing of the SRTM 1 dataset
ALOS PALSAR	12.5	Ellipsoidal	A resample combination of SRTMGL 1 and the US NED and other sources
ACE2	90	Orthometric	A Combination of SRTM and satellite radar altimetry

The first step in the processing strategy concerns the unification of the vertical datums of utilized datasets. The orthometric heights of the collected GNSS/Levelling terrestrial points and heights interpolated from SRTMGL1 GDEM are referenced to the MSL while the PALSAR model produces WGS84-based ellipsoidal heights. Hence, a geoid model is required to unify the vertical datum of all datasets to be MSL-based orthometric heights. This study utilized the Survey Research Institute 2021 geoid model as the most recent most precise local geoid for Egypt (ibid). Thus [24]:

$$H_{PALSAR} = h_{PALSAR} - N_{SRI\,2021} \quad (1)$$

Next, the SRTMGL GDEM has been enhanced based on the concept provided by Rabah et al. [12]. Instead of utilizing the EGM96 GGM in height conversion originally carried out in developing the SRTMGL, the SRI2021 will be used to develop a Modified Egyptian SRTM (MESTTM) as [12]:

$$H_{MESRTM} = H_{SRTMGL} - N_{EGM96} + N_{SRI2021} \quad (2)$$

Next, the four investigated DEMs, namely PALSAR, SRTMGL, ACE2, and MESRTM, have been judged over the available GNNS/Levelling control points. The average and standard deviation of height difference, or DEM errors, for each model, are estimated as:

$$\Delta H_{i,j} = H_{i,j} - H_{DEM} \quad (3)$$

$$\bar{H}_i = \sum Hi \Big/ n \quad (4)$$

$$s_i = \sqrt{\sum (H_{i,j} - \bar{H}_i \Big/ n-1} \quad (5)$$

where,

$H_{i,j}$ is the known orthometric height of a control point no. j,

H_{DEM} is the corresponding orthometric height estimated from a specific DEM,

$\Delta H_{i,j}$ is the ith DEM error in estimating orthometric height for point j,

i range from 1 to 4 investigated models,

$\bar{H}_i$ represents the average height error for the i^{th} DEM,

s_i represents the standard deviation of height error for the i^{th} DEM,

The model producing the best vertical accuracy, in terms of the standard deviation of height differences, will be obtained. Then, its height errors over the control points will be spatially modeled by two approaches. First, the regression analysis statistical toll will be applied to model modelling differences (ΔH) as a function of Easting (Ei) and Northing (Ni) UTM coordinates:

$$\Delta H_{i,j} = a_o + a_1 E_i + a_2 N_i \quad (6)$$

The second modelling approach of DEM errors concerns the utilization of the GIS-based kriging geostatistical analysis. It takes into account the spatial distribution of the sample points to explain the variations in the 3D surface. The general form of the kriging interpolator is [25,26]:

$$\hat{Z}(S_o) = \sum_{i=1}^{n} \lambda_i Z(s_i) \quad (7)$$

where,

$Z(s_i)$ is the measured quantity at the i^{th} location,

λ_i represents an unknown weight for point i,

s_o is the prediction location, and

n equals the measurements number.

Within the ordinary kriging technique, there are many statistical models, or variograms, to model the spatial correlation of datasets. Types of variograms include spherical, circular, exponential, Gaussian and linear.

The results of both modelling steps will be judged over checkpoints to compare their accuracies. Finally, the precise enhanced GDEM will be selected to be applicable for coastal and environmental applications over the study area. The overall processing strategy is depicted in Fig. 1.

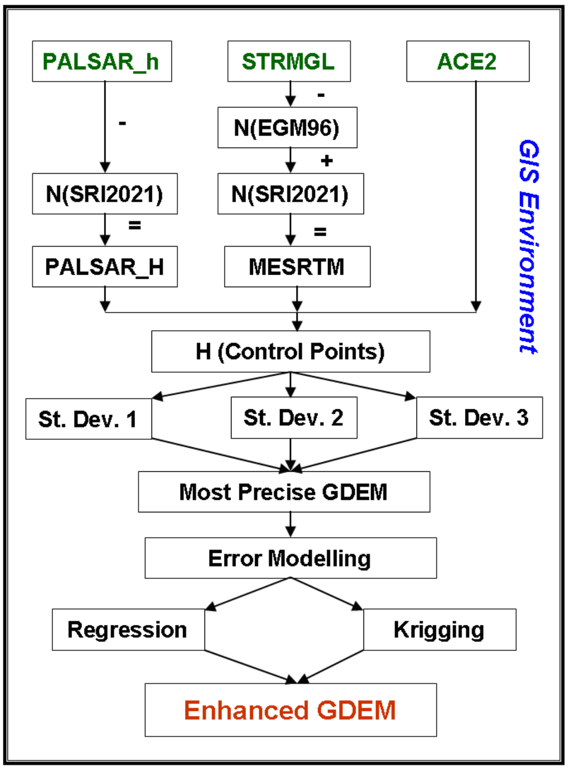

Figure 1. Processing Steps

3. Study Area and Available Data

The study area occupies the Egyptian coasts over the Mediterranean sea from Sallum city at the east to Raffah city at the west (from 25.10 E to 34.20 E) with a variable width equals approximately 25 kilometers (from 30.70 N to 31.60 N). Its overall area equals almost 25,000 square kilometers (Fig. 2). A number of 199 precise-levelling Bench Marks (BM) have been established by the Survey Research Institute (SRI) of the National Water Research Center (NWRC) in the last few years as a part of the Spatial Data Infrastructure (SDI) for coastal and environmental applications. Such BM exist mainly (64%) in the Nile delta region between Alexandria and Port Said cities while there exist 19 BM in the Sinai peninsula and 53 BM in the west coast region. It is worth mentioning that the overall accuracy of both vertical and horizontal coordinates of such a precise geodetic network is less than five centimeters [24]. Twenty-five points (almost 13%) have been reserved as checkpoints to judge the enhanced models' quality. It is worth mentioning that despite the minimal amount of available GNSS/Levelling data points, these datasets comprise the most-accurate geodetic data within the study area.

The three investigated GDEMs, namely, SRTMGL 1, PALSAR, and ACE2, have been downloaded from their particular websites. The Arc GIS 10 software package has been utilized to clip the terrain of the study area from each GDEM model (Fig. 3). The overall heights over the study area range between -72 - 267 m, -54 - 258 m, and -54 - 286 m for the three GDEM models respectively. It can be seen from Fig. 3a that there exist a few gaps in the coverage of the PLASDAR model over the study area particularly at the middle of the Delta and at the far west of the Egyptian boundaries. So, even there exist few BM at such gaps, the study did not include them to have consistency in evaluation the three investigated GDEM models over identical checkpoints.

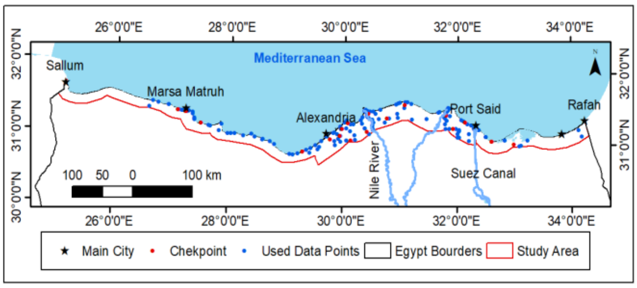

Figure 2. The Study Area and **Available** Data

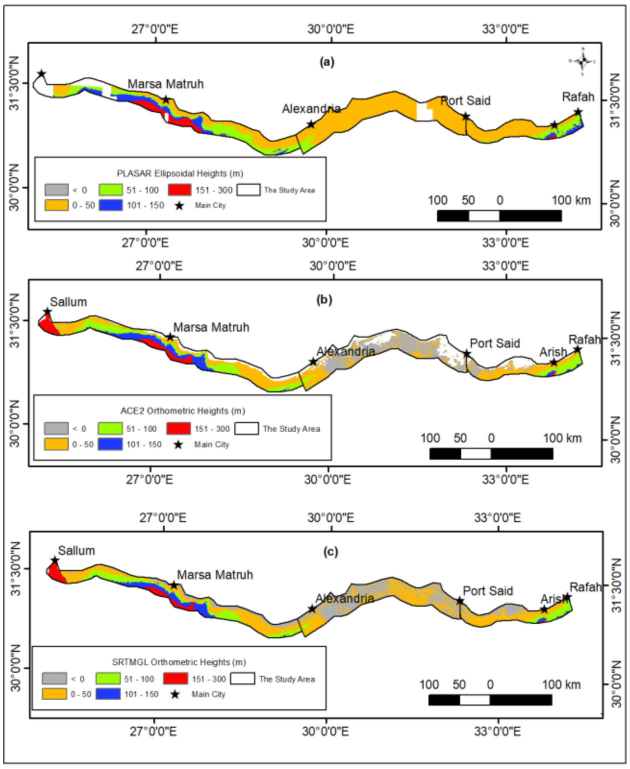

(a) PLASAR, (b) ACE2, and (c) SRTMGL1

Figure 3. The Utilized GDEM Models

4. Results and Discussion

The first step in the data processing stage has been performed to evaluate the vertical accuracy of the original three GDEMs over the available terrestrial precise network. The Arc GIS analysis tools have been carried out to interpolate the GDME-based height at each checkpoint from each GDEM and compare it to the corresponding known height to compute the mean error and standard deviation, using Equations 3 to 5, for all the three GDEMs. Table 2 presents the accomplished findings. It can be realized that, over the known 199 BM, the PALSAR model produced the worst vertical accuracy, in terms of the standard deviation of height differences, while the other two models produced the same level of accuracy. In addition, it can be noticed that the vertical accuracy of the GDEMs, over the Egyptian coasts, equals approximately ± 3 m as other researchers have pointed out in other countries.

Table 2. Statistics of GDEMs-Based Heights Differences at Known Points (m)

	PALSAR	SRTMGL	ACE2
Minimum Height Difference	-24.4	-7.3	-7.7
Maximum Height Difference	4.4	9.1	8.7
Mean Height Difference	-15.21	1.57	1.55
Standard Deviation of Differences	± 3.43	± 2.85	± 2.85

Next, the study obtained two geoid models, namely the global EGM96 model and the local SRI2021 model. The first is used to unify height datums particularly for the PALSAR model (Eq. 1) and the second is used to enhance the performance of the SRTMGL 1 model (Eq. 2). Table 3 presents the statistics of geoidal undulations of both models over the study area. Both models produced almost identical accuracy in height conversion.

Table 3. Statistics of GGMs Geoid Undulations over the Study Area (m)

	EGM96	SRI2021
Minimum Undulation	14.8	14.4
Maximum Undulation	21.2	20.6
Mean Undulation	17.1	16.5
Standard Deviation of Undulation	± 1.4	± 1.4

Thus, equations 1 and 2 have been applied to construct two modified GDEM models: (1) the PLASAR-Ortho producing orthometric heights instead of the original ellipsoidal heights and (2) the Modified Egyptian SRTM (MESRTM) model. The terrain heights over the study area vary between -72 m and 238 m for the MESRTM model and range from -50 m to 266 m for the PLASAR-Ortho model (Fig. 4).

Similarly, the performance of two modified GGMs has been investigated over the terrestrial control points. Table 4 presents the statistics of the accomplished results. Hence, it can be noticed that the vertical accuracy levels equal ± 2.98 m, ± 2.81 m, and ± 2.85 m for the PLASAR-Orth, MESRTM, and ACE2 models respectively.

Comparing Tables 2 and 4, several important notes could be concluded. As expected, it can be concluded that the PALSAR-Orth model is better than the original PLASAR one after converting its height type from ellipsoidal to orthometric types used already in measuring the heights of checkpoints over the study area. Second, the performance of MESRTM model is fairly better than the original SRTMGL 1 model after replacing the height conversion model from the global EGM96 model to the SRI2021 geoid model. That means that such a procedure produced an improvement of almost 1 % over the checkpoints in the study area. Third, it could be realized that the PLASR models (both ellipsoidal and orthometric) produced worse accuracy than the other two investigated GDEMs although its horizontal resolution is small. That might be contributed to its description provided in the last column of Table 1. Accordingly, the remaining procssing steps have been carried out using only MESRTM and ACE2 models.

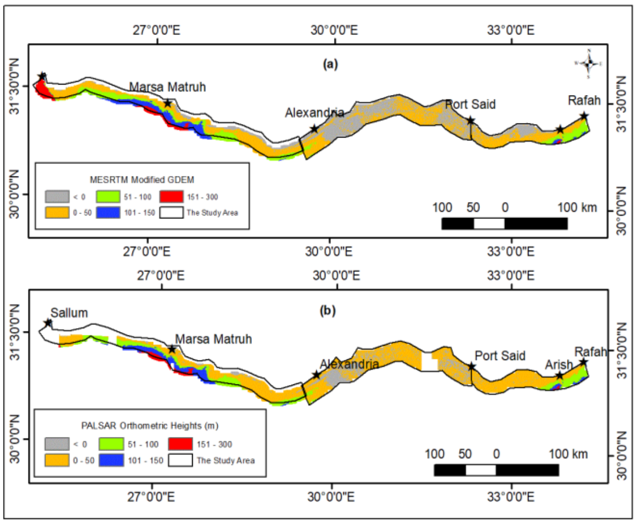

(a) PLASAR Orthometric and (b) MESRTM

Figure 4. The Modified GDEM Models

Table 4. Statistics of Modified GDEMs-Based Heights Differences Known Points (m)

	PALSAR_Ortho	MESRTM	ACE2
Minimum Height Difference	-7.6	-6.7	-7.7
Maximum Height Difference	11.6	10.9	8.7
Mean Height Difference	1.58	2.80	1.55
Standard Deviation of Differences	± 2.98	± 2.81	± 2.85

As noted in the methodology section of this research study, two statistical tools have been applied to model the GDEMs-based errors over the study area. Basically, such tools are based on the regression and krigging approaches. Before performing the regression, 174 available BM have been used in error modelling while the remaining 25 BM (almost 13% of the total number of the accessible dataset) have been kept as checkpoints to evaluate the accomplished results.

First, the linear regression (Eq. 6) has been estimated twice for the two GDEMs models. The attained regression equations are:

$$Error_{MESRTM} = 63.4 - 3.46*10^{-6} E_i - 1.73*10^{-5} N_i \quad (8)$$

$$Error_{ACE2} = -71.3 + 4.55*10^{-6} E_i + 2.07*10^{-5} N_i \quad (9)$$

Then, these two equations have been spatially applied, within the Arc GIS environment, to construct two correction surfaces: CorrMESRTM and CorrACE2. Next, two enhanced GDEM models, namely EnhMESRTM and EnhACE2, have been obtained by adding the original models to the corresponding correction surface:

$$Enh_{MESRTM} = MESRTM + Corr_{MESRTM} \quad (10)$$

$$Enh_{ACE2} = ACE2 + Corr_{ACE2} \quad (11)$$

The GDEMs' corrections (Fig. 5), over the entire study area, range between 1.35 m and 4.19 m for the enhanced MESRTM model and from -0.33 m and 3.28 m for the enhanced ACE2 model.

Likewise, the performance of the two enhanced GGMs has been investigated over the 25 terrestrial control points. Table 5 presents the statistics of the accomplished results. Hence, it can be noticed that the vertical accuracy levels equal ± 2.39 m and ± 2.74 m for the enhanced MESRTM and the enhanced ACE2 models respectively.

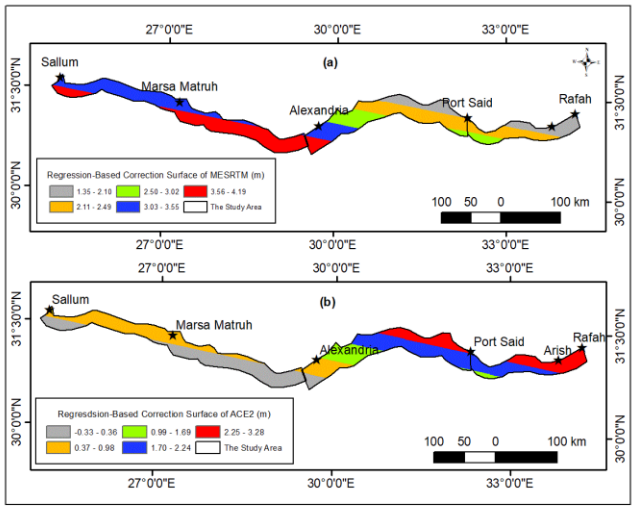

(a) MESRTM and (b) ACE2

Figure 5. The Regression-Based Correction Surfaces of the Enhanced GDEM Models

Table 5. Statistics of Height Differences of Regression-Based Enhanced GDEMs at Known Points

	EnhMESRTM	EnhACE2
Minimum Height Difference	-4.72	-2.81
Maximum Height Difference	4.81	6.77
Mean Height Difference	-0.19	1.77
Standard Deviation of Differences	± 2.39	± 2.74

Comparing Tables 4 and 5, it could be concluded that the regression modelling of height errors has decreased the overall vertical accuracy of the MESRTM model from ± 2.81 m to ± 2.39 m (almost 15% improvements). Similarly, such a modelling approach has decreased the overall vertical accuracy of the ACE2 model from ± 2.85 m to ± 2.74 m (almost 4% improvements only).

The second modelling approach is the kriging statistical tool (Eq. 7) has been applied to model spatially the errors of the GDEMs over the study area. Correspondingly, other two correction surfaces have been obtained for the MESRTM and ACE2 models. The corrections, over the entire study area, range between -0.337 m and 5.215 m for the MESRTM model and from -2.227 m and 4.703 m for the ACE2 model. Later, each correction surface has been added to the corresponding original GDEM to obtain the kriging-based enhanced version, over the study area, explicitly the Enh_2_MESRTM and the Enh_2_ACE2 models (Fig. 6).

Finally, the vertical accuracy of those two models has been judged over the 25 checkpoints. The accomplished results are tabulated in Table 6, which shows that the overall accuracy of the MESRTM model has been decreased from ± 2.81 m to ± 2.15 m and that of the ACE2 model has been decreased from ± 2.85 m to ± 2.40 m. Thus, it can be concluded that the kriging-based enhanced versions of the two GDEMs have improvements equal 24% and 16% for the MESRTM and ACE2 models respectively.

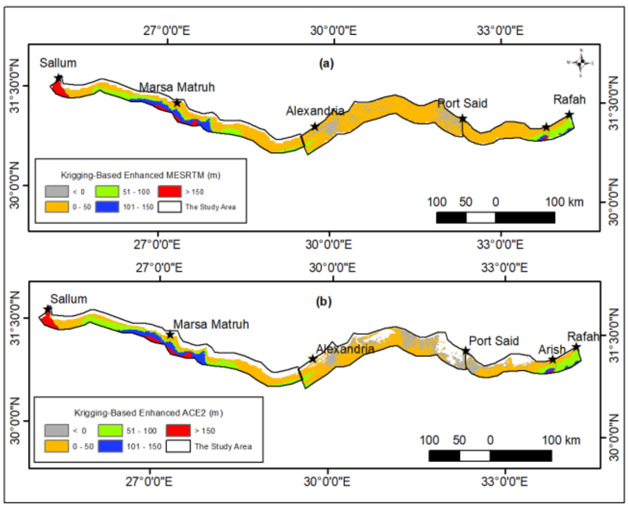

(a) Enh_2_MESRTM and (b) Enh_2_ACE2

Figure 6. The Kriging-Based Enhanced GDEM Models

Table 6. Statistics of Height Differences of Kriging-Based Enhanced GDEM at Known Points

	Enh_2_MESRTM	Enh_2_ACE2
Minimum Height Difference	-6.282	-3.959
Maximum Height Difference	3.246	4.552
Mean Height Difference	-0.429	0.888
Standard Deviation of Differences	± 2.15	± 2.40

Comparing the results of both modelling approaches, it has been found that the regression method produced improvements of 15% and 4% for the investigated MESRTM and ACE2 models respectively. On the other hand, the attained improvements equal 24% and 16% for the same GDEMs. That concludes that the kriging geostatistical modelling is better than the regression method since it takes the spatial correlation between the data points.

Regarding the utilization of different variogram types within the kriging process, five variograms have been utilized in the development of kriging-based enhanced GDEMs, namely the spherical, circular, exponential, Gaussian, and linear variograms. The accomplished results were very close within the centimeter-level in terms of both mean and standard deviation. However, such insignificant findings could be due to the study area’s small size and the limited number of datasets available. As a result, the role of variogram types in enhancing GDEMs should be studied more thoroughly over wider spatial regions and with more data points.

The current study not only evaluates the performance of GDEMs as various previous researches but extends its objectives to enhance such global models by incorporating more terrestrial local datasets. It is a matter of reality that, in many developing countries, there are no accessible precise DEMs and the utilization of low-accuracy GDEMs is the affordable cost-effective alternative. Thus, enhancing the performance of GDEMs is valuable for environmental and mapping activities. The current research addresses this need by presenting a straightforward GIS-based solution. However, because of the limited number of attainable terrestrial data points, such a technique should be thoroughly examined in other larger areas with a sufficient number of data points.

5. Conclusions

Global Digital Elevation Models provide open-source free-of-charge accessible data to represent the topography of a spatial area. Such models have been developed and distributed worldwide and have been extensively applied in several coastal management and environmental applications. It is a matter of reality that each activity requires a certain level of vertical accuracy to meet its requirements and specifications. The current research investigates the vertical accuracy of different resolution GDEMs (namely PALSAR, SRTMGL 1, and ACE2) over the 1000-kilometrs Egyptian coasts along the Mediterranean sea using accurate GNSS/Levelling datasets. The vertical datum of those models has been first unified and a local geoid model has been utilized for height conversion. In addition, the study tries to enhance such accuracy levels by adding terrestrial precise datasets and utilizing both the regression and the kriging statistical methods to spatially model the GDEM-based height errors.

Based on the available datasets, few conclusions have been drawn. Being judged over terrestrial precise BM, the vertical accuracy of the original GDEMs be ± 3.43 m for the PALSAR model and ± 2.85 m for both SRTMGL 1 and ACE2 models. Converting the PLASAR vertical datum from the WGS84 one to the MSL datum reduce its vertical accuracy to 2.98 m over the available ground points.

Replacing the utilized geoid model used in height transformation of the SRTMGL 1 model, from the global EGM96 geoid to the local SRI2021 one, enhance its accuracy a little bit. Applying the regression modelling method results in enhancing the vertical accuracy of MESRTM and ACE2 by 15% and 4% respectively. On the other hand, the kriging geostatistical method produced 24% and 16% improvements for the MESRTM and the ACE2 respectively. Accordingly. It is concluded that the kriging geostatistical modelling is better than the regression method since it takes the spatial correlation between the data points.

According to the accomplished findings, few significant concluding remarks could be summarized. First, the presented approach of adding terrestrial local BM datasets to a global DEM could considerably increase its overall vertical accuracy. Second, the number of added terrestrial points should be appropriate to the desired level of vertical accuracy and the area of study. For instance, 200 BM have been added in the current research study to decrease the overall accuracy of a particular GDEM from ± 2.85 m to ± 2.15 m over the current study area. Thus, it might be concluded that enhancing the accuracy of GDEMs to a sum-meter level may require collecting a huge number of BM, which is obviously expensive. Third, the achieved vertical accuracy of the enhanced models, herein, could be suitable for small-scale mapping, hydrological investigations, and overall management of coastal regions. However, it might not be appropriate for accurate environmental studies such as Sea Level Rise (SLR) monitoring and risk assessment which requires accurate DEM for representing the topography of a particular area.

Declaration of Interest Statement

No potential interest was reported by the authors.
No funding was allocated for this research.

REFERENCES

[1] Khasanov, K. and Ahmedov, A. (2021). Comparison of digital elevation models for the designing water reservoirs: a case study of Pskom water reservoir, *E3S Web of Conferences*, 264, 03058, doi:10.1051/e3sconf/202126403058.

[2] Al-Krargy, E. and Dawod, G. (2021). Optimum combinations of GGM and DEM models for precise national geoid development, *Proceedings of Engineering and Technology Innovation*, V. 18, pp. 15-24, doi:10.46604/peti.2021.6452.

[3] Dawod, G. and Ascoura, I. (2021). The Validity of open-source elevations for different topographic map scales and geomatics applications, Journal of Geographic Information System, V. 13, No. 2, pp. 148-165.

[4] Khalil, H. and Hassaan, M. (2017). Developing a reliable digital elevation model for climate change applications, case study: the Nile delta, *Alexandria Research Center for Adaptation to Climate Change (ARCA) working paper No. 6*, Alexandria University, Alexandria, Egypt.

[5] Sumanathna, A., Madurapperuma, B., Hangawatta, T., Pathirage, I., and Fernando, G. (2018). Developing coastal Digital Elevation Model (DEM) to indicate tsunami flooding topography in Arugam bay, Sri Lanka, *Proceedings of the Institute of Professional Studies and Skills Development (IPSSD) Grand Day Online Conference*, pp. 1-14.

[6] Wahid, A., Madden, M., Khalaf, F., and Fathy, I. (2016). Geospatial analysis for the determination of hydro-morphological characteristics and assessment of flash flood potentiality in arid coastal plains: A case in southwestern Sinai, *Egypt, Earth Sciences Research Journal*, 20(1), E1-E9, https:// doi.org/10.15446/esrj.v20n1.49624.

[7] Gaber, A., Darwish, N., and Koch, M. (2017). Minimizing the residual topography effect on interferograms to improve DInSAR results: Estimating land subsidence in Port-Said city, Egypt, *Remote Sensing*, 9, 752, doi:10.3390/rs9070752.

[8] Abdel-Aziz, T., Dawod, G., and Ebaid, H., (2020). DEMs and reliable sea level rise risk monitoring in Nile Delta, Egypt, Discover Sustainability, V. 1, No. 1, doi:10.1007/s43621-020-00006-7.

[9] Patel, A., Katiyar, S. and Prasad, V. (2016). Performance evaluation of different open source DEM by Differential Global Positioning System (DGPS), *The Egyptian Journal of Remote Sensing and Space Sciences*, No. 19, pp. 7-16.

[10] Kulp, S. and Strauss, B. (2016). Global DEM Errors under predict coastal vulnerability to sea level rise and flooding, *Frontiers in Earth Science*, 4:36. doi:10.3389/feart.2016.00036.

[11] Dawod, G. and Al-Ghamdi. K. (2017). Reliability of recent global digital elevation models for geomatics applications in Egypt and Saudi Arabia, *Journal of Geographic Information System*, V. 9, No. 6, pp. 685-698.

[12] Rabah, M., El-Hattab, A. and Abdallah, M. (2017). Assessment of the most recent satellite based digital elevation models of Egypt, *NRIAG Journal of Astronomy and Geophysics*, doi:10.1016/j.nrjag.2017.10.006.

[13] Mukherjee, S., Joshi, P., Mukherjee, S., and Ghosh, A. (2013). Evaluation of vertical accuracy of open source Digital Elevation Model (DEM), *International Journal of Applied Earth Observation and Geoinformation*, No. 21, pp. 205-217.

[14] Ouerghi, S., Abdalla ELsheikh, R. Achour, H. and Bouazi, S. (2015). Evaluation and Validation of Recent Freely-Available ASTER-GDEM V.2, SRTM V.4.1 and the DEM Derived from Topographical Map over SW Grombalia (Test Area) in North East of Tunisia, *Journal of Geographic Information System*, No. 7, pp. 266-27.

[15] Leon, J., Heuvelink, G., and Phinn, S. (2014). Incorporating DEM uncertainty in coastal inundation mapping, *PLoS ONE*, V. 9, No. 9: e108727, doi:10.1371/journal. pone.0108727.

[16] Hu, Z., Peng. J., Hou, Y. and Shan, J. (2017). Evaluation of Recently Released Open Global Digital Elevation Models of Hubei, China, *Remote Sensing*, 9, 262; doi: 10.3390/rs9030262.

[17] Wang, X., Holland, D., and Gudmundsson, H. (2018). Accurate coastal DEM generation by merging ASTER GDEM and ICESat/GLAS data over Mertz Glacier, Antarctica, *Remote Sensing of Environment*, No. 206, pp.

218-230.

[18] *Abd-Elmotaal, H., Abd-Elbaky, M. and Ashry, M. (2013). 30 Meters Digital Height Model for Egypt,* Presented at the VIII Hotine-Marussi Symposium, *June 17-22, Rome, Italy*.

[19] Jamali, A., Mustapha, A., and Mostafa, S. (2021) Prediction of sea level oscillations: Comparison of regression-based approach, *Engineering Letters*, V. 29, No. 3, pp. 1-6.

[20] Orejuela, I., Gonzalez, C., Guerra, X., Mora, E., and Toulkeridis, T. (2021) Geoid undulation modeling through the Cokriging method - A case study of Guayaquil, Ecuador, *Geodesy and Geodynamics*, No. 12, pp. 356-367.

[21] USGS (The US Geological Survey), (2022). *SRTMGL1 V003*, Available at: https://lpdaac.usgs.gov/products/srtmgl1v003/, Accessed 6 Jan, 2022.

[22] ASF (Alaska Satellite Facility) (2022). *ALOS PLASAR – Radiometric Terrain Correction*, https://asf.alaska.edu/data-sets/derived-data-sets/alos-palsar-rtc/alos-palsar-radiometric-terrain-correction/, Accessed 6 Jan, 2022.

[23] Smith, R. and Berry, P. (2019). *Altimeter Corrected Elevations, Version 2 (ACE2)*, A Technical Report, 22p, Columbia University, New York, USA.

[24] SRI (Survey Research Institute) (2018). *Establishing accurate geodetic networks along the Egyptian coastlines*, Internal Technical Report, No. 1.

[25] Brimicombe, A. (2010). GIS, *environmental modeling and engineering*, Second Edition, CRC Press, New York, USA, 361 pp.

[26] ESRI (Environmental Systems Research Institute) (2021). *How krigging works*, https://desktop.arcgis.com/en/arcmap/10.3/tools/3d-analyst-toolbox/how-kriging-works.htm, Accessed 12 Dec, 2021.